Activation of G protein-coupled receptors : the role of extracellular loops in adenosine receptors

Peeters, M.C.

CHAPTER 4

THREE "HOTSPOTS" IMPORTANT FOR ADENOSINE A_{2B} RECEPTOR ACTIVATION: A MUTATIONAL ANALYSIS OF TRANSMEMBRANE DOMAINS 4 AND 5 AND THE SECOND EXTRACELLULAR LOOP

This chapter was based upon:

M.C. Peeters, Q. Li, G.J.P. van Westen, A.P. IJzerman. Purinergic Signaling **2011** [In press]

ABSTRACT

G protein-coupled receptors (GPCRs) are a major drug target and can be activated by a range of stimuli, from photons to proteins. Despite the progress made in the last decade in molecular and structural biology, their exact activation mechanism is still unknown. Here we describe new insights in specific regions essential in adenosine A_{2B} receptor activation ($A_{2B}R$), a typical class A GPCR. We applied unbiased random mutagenesis on the middle part of the human adenosine A_{2B} receptor ($A_{2B}R$), consisting of transmembrane domains four and five (TM4 and TM5) linked by extracellular loop 2 (EL2), and subsequently screened in a medium-throughput manner for gain-of-function and constitutively active mutants (CAMs). For that purpose we used a genetically engineered yeast strain (*S. cerevisiae* MMY24) with growth as a read-out parameter. From the random mutagenesis screen, 12 different mutant receptors were identified that form three distinct clusters; at the top of TM4, in a cysteine-rich region in EL2, and at the intracellular side of TM5. All mutant receptors show a vast increase in agonist potency and most also displayed a significant increase in constitutive activity. None of these residues are supposedly involved in ligand binding directly. As a consequence, it appears that disrupting the relatively 'silent' configuration of the wild-type receptor in each of the three clusters readily causes spontaneous receptor activity.

INTRODUCTION

The adenosine receptors form a small subfamily of class A G protein-coupled receptors (GPCRs). Four subtypes of adenosine receptors are known (A_1R, $A_{2A}R$, $A_{2B}R$, and A_3R) that all bind the endogenous ligand adenosine. The A_1R and the A_3R subtypes are coupled to G_i proteins, hereby mediating the inhibition of adenylyl cyclase causing decreased levels of cAMP in the cell. The $A_{2A}R$ and $A_{2B}R$ signal mainly through G_s proteins resulting in the activation of adenylyl cyclase and an increase in intracellular cAMP levels. Of the adenosine subfamily, the $A_{2B}R$ subtype has been investigated least. Similar to all GPCRs, the $A_{2B}R$ is made up of seven transmembrane domains connected by three intracellular and three extracellular loops, an extracellular N-terminus, and an intracellular C-terminus. The adenosine A_{2B} receptor ($A_{2B}R$) has been implicated in several (auto)-immune diseases such as asthma and chronic obstructive pulmonary disease (COPD) and is therefore an interesting drug target [1].

In a previous study, random mutagenesis combined with a yeast screen for activating mutant receptors have been performed on two parts of the adenosine A_{2B} receptor in order to identify specific residues involved in the activation of the receptor [2,3]. Mutations were randomly introduced in two separate fragments of the receptor, one ranging from the ATG until a KpnI restriction site in the second intracellular loop and a second form the BglII restriction site in the third intracellular loop until the end of the receptor (**Figure 1**). These studies revealed many constitutively active mutations, both in the transmembrane domains as well as in the extracellular regions. The fragment that is in between the two restriction sites KpnI and BglII, encompassing transmembrane domain 4 (TM4), the second extracellular loop 2 (EL2), and transmembrane domain 5 (TM5), has so far not been examined. However, this region may be very important in the activation mechanism of the receptor. All three domains in this fragment have been implied to participate in the dynamic movements the receptor undergoes during activation [4]. Clear evidence for the importance of this region is also provided by the recently published crystal structures of both the antagonist-bound and agonist-bound adenosine $A_{2A}R$, the closest homologue of the $A_{2B}R$. In particular EL2 and TM5 appear to be involved directly in ligand binding and in conformational movements induced by agonist binding [5,6,7]. Also, EL2 has been

proposed to act as a negative regulator for the receptor, keeping it in its inactive state and is in many receptors part of the ligand binding site [8,9,10,11].

In the present study we examined the influence of EL2 and its two adjacent transmembrane domains, TM4 and TM5, of the adenosine A_{2B} receptor on receptor activation. We performed an unbiased random mutagenesis screen for gain-of-function mutations as well as constitutively active mutants (CAMs) , i.e. mutant receptors that show basal activity independent of an agonist. In these CAMs, the equilibrium between the inactive (R) and active conformation (R*) is shifted, so that the active state is energetically more favorable than in the wild type situation, similar to what occurs when the receptor binds an agonist [12]. Residues that are mutated to cause this shift in equilibrium are therefore likely to be involved in the on-and-off switch of the receptor and can provide us with information on the activation mechanism of the receptor.

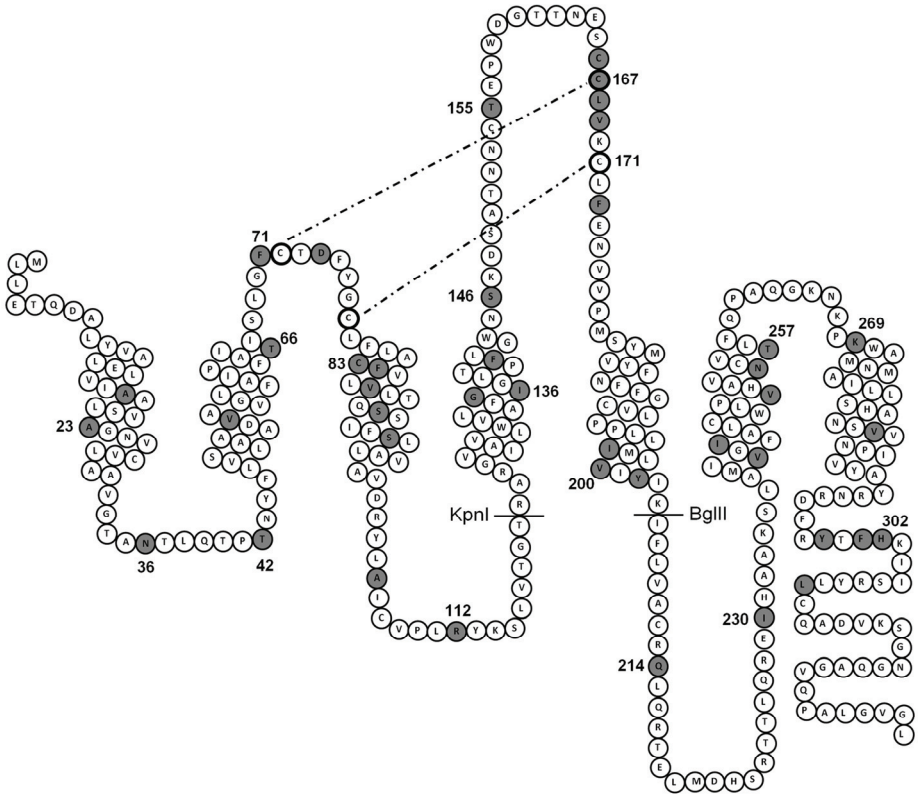

Figure 1. Snake-plot of the adenosine A_{2B} receptor. Mutated residues within the A_{2B}R identified to result in increased constitutive activity are indicated in grey. These mutations originate from two previously described screens. and the TM4-EL2-TM5 screen described in the current paper. The putative disulfide bridges are indicated with dotted lines. The disulfide bridge conserved in many class A GPCRs links $C78^{3.25}$ and $C171^{EL2}$. The non-conserved second disulfide bridge between EL1 and EL2 is based on an analogous bond in the crystal structures of the adenosine A_{2A}R (PDB: 3EML, 3QAK, 3YDO, 3YDV); it links $C72^{EL1}$ and $C167^{EL2}$. The restriction sites KpnI and BglII are indicated; they were used to obtain the fragment for random mutagenesis

We performed the screen for activating mutant receptors using a *S. cerevisiae* strain that has been genetically modified to serve as a reporter system with growth as an output parameter. This yeast system is an ideal background to monitor activation of a single GPCR, since the endogenous GPCR (Ste2) has been removed from the system while still maintaining the complete GPCR signaling machinery [13]. Several previous reports have proved this eukaryotic system to be predictive of the mammalian situation, as shown by functional and binding studies in CHO cells [2,14]. Several mutated residues were identified, causing the receptor to be highly increased in both agonist-induced and spontaneous activity. The results presented here can be of general interest in increasing our understanding of the activation mechanism of class A GPCRs, of adenosine receptors in particular as well as other members of this superfamily.

MATERIALS AND METHODS

DNA Constructs

The S*. cerevisiae* expression vector containing the adenosine A_{2B} receptor gene, the pDT-PGK_A_{2B}R plasmid, was kindly provided by Dr. Simon Dowell from GSK (Stevenage, UK). A KpnI restriction site was introduced in the A_{2B}R gene in the region encoding the second intracellular loop. Together with a restriction site in the third intracellular loop, BglII, it is possible to divide the receptor into three large fragments suitable for random mutagenesis. The fragment between these two restriction sites was used in the mutagenic PCR. This fragment encodes transmembrane domain four, the second extracellular loop, and transmembrane domain five (TM4-EL2-TM5).

Mutagenic PCR for the construction of the random mutagenesis library

The introduction of random mutations in the adenosine A_{2B} receptor was achieved by manipulating the polymerase chain reaction adapted from the method of Fromant et al. [15]. In this error-prone PCR method, the balance between Mg^{2+} ions and Mn^{2+} ions was shifted, compromising fidelity of the DNA polymerase enzyme. Furthermore, the introduction of mutations can be guided by adding excess of one of the nucleotides (the ‘forcing’ nucleotide). This technique makes it possible to

introduce mutations in fragments up to 400 bp in length. The DNA fragment encoding TM4-EL2-TM5 encompasses 262 bp. The mutagenic reaction contained 10 ng of template DNA, 0.1 µM concentrations of each primer, 0.2 mM concentrations of dNTPs as well as 3.4 mM concentrations of the nucleotide in excess dCTP, 0.5 mM $MnCl_2$, 4.7 mM $MgCl_2$, and 0.5 units of Super *Taq* polymerase without proofreading. The number of mutagenic PCR cycles was set to 10. Using these conditions, only a limited amount of mutations are introduced per fragment [16].

The following primers were used:

5'-GGTATAAAAGTTTGGTCACGGGTACCCGAGCAA-3'

5'-GAAGCTGCCTGCAGGCCACCAGGAAGATCTTAATG-3'

The mutagenic PCR products were submitted to agarose gel electrophoresis and the gel bands containing the mutated fragments were isolated from the gel and purified. Subsequently, the mutated fragments were amplified further with 10 cycles of a regular PCR with the same primer sets. After the error prone PCR, the normal fragment TM4-EL2-TM5 in the wild type receptor was replaced by the mutated fragments using the restriction sites KpnI and BglII and transformed into DH5α *E.Coli* competent cells (Invitrogen, San Diego, CA, USA). Plasmids were isolated from the culture resulting in a mutagenic adenosine A_{2B} receptor library.

Transformation in MMY24 S. cerevisiae strain

pDT-PGK_A_{2B}R plasmids were transformed into an *S. cerevisiae* yeast strain according to the Lithium-Acetate procedure [17]. The MMY24 strain is derived from the MMY11 strain and was further adapted to communicate with mammalian GPCRs through the introduction of a chimeric G protein [13]. The genotype of the MMY24 strain is: *MAT**a**his3 leu2 trp1 ura3can1 gpa1_::G_i3 far1 ::ura3 sst2_::ura3 Fus1::FUS1-HIS3 LEU2::FUS1-lacZ ste2_::G418R.* To measure signaling of GPCRs, the pheromone signaling pathway of this strain was coupled via the FUS1 promoter to HIS3, a gene encoding the key enzyme in histidine production, imidazole glycerol-phosphate dehydrase. The degree of receptor activation was measured by the growth rate of the yeast on histidine-deficient medium. A second reporter gene was placed under control of the FUS1 promoter; the LacZ gene. Transcription of this gene results in the production of the enzyme β-galactosidase. The presence of this enzyme is also a measure of receptor activation.

Random mutagenesis screen

The random mutagenesis screen was performed on selection agar medium in two steps. Firstly, yeast cells were selected for the presence of the plasmid pDT-PGK using selection medium lacking the markers uracil and leucine (YNB-UL). After 3 days of incubation at 30 ˚C, positive colonies were pooled. For the second selection step, 10^4 cells were spread onto selection medium lacking uracil, leucine, and histidine (YNB-ULH) to select for the pDT-PGK plasmid, the MMY24 yeast strain, and activity of the receptor, respectively. A concentration of 7 mM 3-aminotriazole (3-AT), a competitive inhibitor of imidazole glycerol-phosphate dehydrase, was added to the agar plates to suppress basal yeast growth that occurs in histidine-deficient medium. Also, a concentration of 1 nM of the full $A_{2B}R$ agonist 5'-*N*-ethylcarboxamido-adenosine (NECA) was added to the medium, a concentration at which yeast cells expressing the wild type human adenosine A_{2B} receptor still barely grow. After three days, colonies were selected and transferred to new selection plates. To further select for true active mutant receptors, we performed a qualitative β-galactosidase assay according to protocol #PT3024-1 from Clontech (Clontech laboratories, Mountain View, California). In brief, yeast colonies were transferred to a filter and lysed using repeated freeze-thawing with liquid nitrogen. The filter was then placed on top of several Whatman papers presoaked in Z-buffer (16.1 g/L Na_2HPO_4, 5.5 g/L NaH_2PO_4, 0.75 g/L KCl, 0.246 g/L $MgSO_4$, 0.3% β-mercaptoethanol) and 0.3 mg/ml X-gal (5-bromo-4-chloro-3-indolyl-β-D-galactosidase), a substrate of β-galacto-sidase. The filter was incubated at 30ºC until a blue color appeared. Colonies with a blue color were chosen for further characterization. Mutated receptors were sequenced and subsequently retransformed into the yeast strain to confirm their activated phenotype.

Liquid growth assay

To characterize the mutant receptors further, concentration-growth curves were generated in a liquid growth assay. This assay is on 96-wells scale and growth is easily determined by measuring absorption at a wavelength of 595 nm. In this assay, 150 µl liquid YNB-ULH medium with 7 mM 3-AT and a varying concentration of NECA (10^{-10}-10^{-5} M) was added to each well. A concentration range from 10^{-10} to 10^{-5} M was also used for the concentration-growth curves with BAY 60-6583 (2-[6-amino-3,5-dicyano-4-[4-(cyclopropylmethoxy)phenyl]pyridin-2-ylsulfanyl]acetamide;

synthesized in house), a non-nucleoside agonist [18]. Yeast cells from an overnight culture were diluted to around $4 \cdot 10^6$ cells/ml ($OD_{600} \approx 0.2$) and 50 µl was added per well. The 96-wells plate was then incubated for 35 hours in a Genios plate reader (Tecan, Durham, NC). at 30°C, keeping the cells in suspension by shaking every 10 minutes at 300rpm for 1 minute. Results originate from three independent experiments, performed in duplicate.

Solid growth assay

To monitor the response of the mutant receptors in the presence of the inverse agonist ZM241385 (4-{2-[7-amino-2-(2-furyl)[1,2,4]triazolo-[2,3-a][1,3,5]triazin-5-yl-amino]ethyl}phenol), a solid yeast growth assay was used. Yeast growth was determined based on growth density, rather than absorption at 595 nm; this enabled us to visualize the level of constitutive activity more clearly. In the solid growth assay, yeast cells from an overnight culture were diluted to around 400,000 cells/ml (OD600 ≈ 0.02), and droplets of 1.5 µl were spotted on selection agar plates, YNB-ULH, containing 7 mM 3-AT and a ZM241385 concentration ranging from 10^{-11} to 10^{-5} M. For the single point experiments, a final concentration of 10^{-5} M ZM241385 was used [19]. After incubation at 30°C for 50 h, the plates were scanned and receptor-mediated yeast growth was quantified with Quantity One imaging software from Bio-Rad (Hercules, CA). The growth rate of yeast was calculated as the density of each spot with a correction for local background on the plate. Results are obtained from four independent experiments, performed in quadruplicate.

Whole cell radioligand binding experiments

Yeast cells expressing wild type or mutated A_{2B}Rs were cultured overnight in rich YAPD (Yeast Extract Adenine Peptone Dextrose) medium. Cells were centrifuged for 5 minutes at 2000 xg, the pelleted cells were once washed with 0.9% NaCl. The cells were again centrifuged 5 minutes at 2000 xg and diluted in the assay buffer (50mM Tris-HCl pH7.4 + 1mM EDTA) to OD_{600}=40 ($OD_{600} = 1 \approx 2.5 \cdot 10^7$ cells/ml). Binding experiments were performed with 1.3 nM [^{3}H]PSB-603 (8-[4-[4-(4-Chlorophenyl) piperazine-1-sulfonyl)phenyl]]-1-propylxanthine; $K_{D,yeast}$ = 0.8 +/- 0.02 nM) and a final cell concentration of $25 \cdot 10^7$ cells/ml in a total volume of 100 µl [3,20]. Nonspecific binding was determined in the presence of 1mM NECA. For whole competition

curves a concentration range of 10^{-10}-10^{-3} M of the ribose agonist NECA, 10^{-10}-10^{-4} M of the non-ribose agonist BAY 60-6583, or 10^{-10}-10^{-4} M of the inverse agonist ZM241385 was used. Samples were incubated for 1 hour at 25ºC while shaking vigorously to keep the yeast cells in suspension. Incubation was terminated by adding 1ml ice-cold assay buffer. Bound from free radioligand was immediately separated by rapid filtration through Whatman GF/B filters pre-incubated with 0.1% polyethylenimine (PEI) using a Millipore manifold during which the filters were washed six times with ice-cold assay buffer. Filter-bound radioactivity was determined by scintillation spectrometry (Tri-Carb 2900TR; PerkinElmer Life and Analytical Sciences) after addition of 3.5 ml of PerkinElmer Emulsifier Safe. Results are obtained from three independent experiments, performed in duplicate.

Whole cell extracts and immunoblotting

Whole protein cell extracts were made from the transformed yeast cells using trichloroacetic acid (TCA). From an overnight culture, $1.2 \cdot 10^8$ yeast cells were harvested in mid-log phase. The cells were washed twice with 20% TCA after which they were broken by vigorous vortexing in the presence of glass beads. The yeast cell extracts were separated using SDS/PAGE and subsequently blotted on Hybond-ECL membranes. For this purpose, a sample of 4.0 µl containing 12 µg protein was loaded on a 12.5% SDS/PAGE gel. A semi-automated electrophoresis technique (PhastSystem™, Amersham Pharmacia Biotech) was used for SDS/PAGE as well as blotting. The antibody directed against the C-terminal region of the adenosine A_{2B} receptor was kindly provided by Dr. I. Feoktistov (Vanderbilt University, Nashville). Densitometric analysis of the protein bands was performed using the volume analysis tool as present in the Quantity One imaging software from Bio-Rad (Hercules, CA). The non-specific band at approximately 45 kDa was used as loading control. The ratio between specific $A_{2B}R$ protein bands (at 29 kDa and 48 kDa) and the non-specific band was determined and the wild type receptor was set at 100%, the empty vector pDT-PGK at 0%. The experiment was performed in duplicate. The relative expression levels represent expression of the whole receptor population, not distinguishing between cell surface and intracellularly expressed protein.

Bioinformatics - Mapping the mutated residues onto the adenosine A_{2A} receptor structure

The positions of the mutations identified in the random mutagenesis screen were mapped onto the corresponding positions in the crystal structure of the agonist-bound adenosine A_{2A} receptor (PDB: 2YDV) [7]. These corresponding positions were determined by a multiple sequence alignment created using ClustalW with default parameters. To make use of known crystallographic data, the sequences of the CXCR4 Chemokine (CXCR4R) receptor and the β_2-adrenergic (b2AR) receptor were included in this alignment. The EL2 was defined from the crystal structures of the A_{2A} receptor (residues 143 to 173), the CXCR4R (residues 175 to 192) and the b2AR (residues 171 to 196). The amino acids in the TM domains of the various receptors were related through their Ballesteros and Weinstein numbering [21].

Bioinformatics - cysteine occurrence analysis

To gain insight in the number of class A GPCRs that have multiple cysteines present in the second extracellular loop, we analyzed all human olfactory (415) and non-olfactory (221) class A GPCRs as present in the GPCRDB [22]. A cysteine count was performed on the second extracellular loop that for this analysis was defined as the fragment between residues 4.55 and 5.38 according to the Ballesteros and Weinstein numbering [21]. These two residues are located at the interface of the loop and the transmembrane domains, but are present within the membrane in all predictions.

RESULTS

Random mutagenesis screen in yeast

Mutations were randomly introduced in the fragment encoding for transmembrane domain 4 (TM4), the second extracellular loop (EL2), and transmembrane domain 5 (TM5) of the human adenosine A_{2B} receptor using an error-prone PCR reaction (**Figures 1 and 2**). The corresponding fragment in the wild type receptor was replaced after mutagenesis by the mutated fragments, which rendered a set of approximately 5000 different plasmids of which ca. 80% contained mutations. The mutations occurred in a low frequency; most of the mutant receptors contained single point mutations and the mutant receptor with the highest mutation frequency

contained 5 nucleotide changes. These results are comparable to a random mutagenic library of the first three transmembrane domains of the $A_{2B}R$ published by Beukers et al. [2]. After ligation, the plasmids were propagated in competent *E. coli* cells, resulting in the final mutant $A_{2B}R$ library (**Figure 2**). This mutant library was subsequently transformed in the *S. cerevisiae* MMY24 strain.

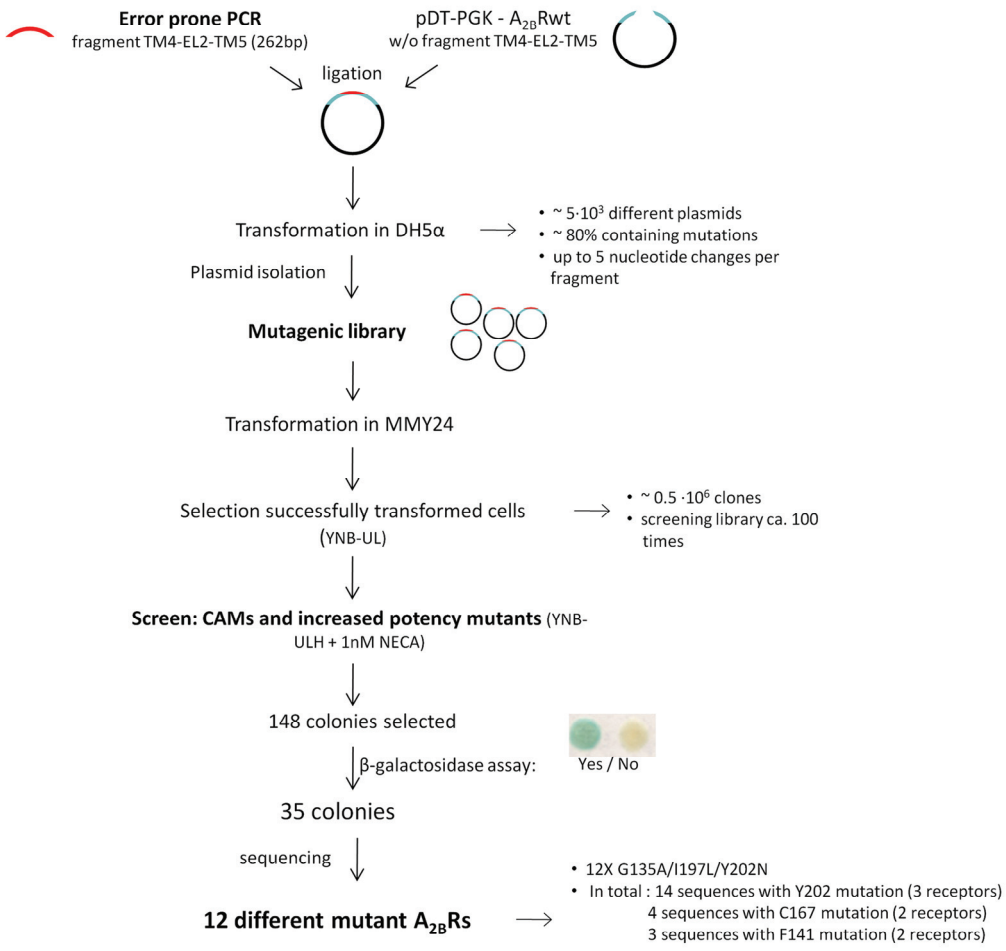

Figure 2. Schematic overview of the screen for activating mutations. The mutated fragments from the mutagenic PCR were reintroduced in an otherwise wild type $A_{2B}R$ in the pDT-PGK vector, resulting in the mutagenic $A_{2B}R$ library. The library was transformed in the MMY24 yeast strain and screened for mutant receptors with constitutive activity and/or an increased potency for NECA. As a second selection criteria, the presence of β-galactosidase was determined in a qualitative assay, resulting in a final selection of 35 yeast colonies. Sequencing revealed 12 different mutant receptors.

The MMY24 yeast strain has been genetically modified to enable mammalian GPCRs to couple to the yeast pheromone pathway with subsequent transcription of the reporter gene HIS3, increasing the histidine synthesis. We used this trait to specifically select yeast cells that express an active receptor by their ability to produce histidine and therefore grow on histidine-deficient medium. Before starting

the actual screen, we first selected yeast cells that were successfully transformed. We then screened the transformed MMY24 cells for an active phenotype on selection plates lacking uracil, leucine, and histidine (YNB-ULH) to select for the MMY24 yeast strain, the pDT-PGK plasmid, and activity of the receptor, respectively. By also adding a low concentration of 1 nM of the agonist NECA (EC_{50} value at wild type $A_{2B}R$: 137 +/- 10 nM, see also **Table 1**), we screened for both constitutively active mutants (CAMs) and mutant receptors with increased agonist potency. In total, ca. 0.5 million yeast clones were used for the final activation screen, so the library was screened approximately 100 times. From the screen, all well separated colonies that appeared on the selection plates were selected (a total of 148 yeast colonies). Besides the reporter gene HIS, a second reporter gene was incorporated into the MMY24 genome under the same promoter; the LacZ reporter gene, causing the yeast cell to also produce the enzyme β-galactosidase. To proceed with the most active mutant receptors, we performed a qualitative β-galactosidase assay. The colonies were lysed and the presence of the enzyme β-galactosidase was measured. The 35 colonies with the strongest response in this assay, out of the original 148, were selected, plasmids were isolated from the yeast cells and the mutations were identified by sequencing. Several of the nucleotide changes observed in the sequences resulted in the same amino acid changes in the $A_{2B}R$. Mutant receptor G135A$^{4.55}$/I197L$^{5.53}$/Y202N$^{5.58}$ was identified most, namely 12 times out of the 35 sequenced plasmids (shown in superscript are the positions according to the Ballesteros and Weinstein GPCR numbering system [21]) (**Figure 2, Table 1**). In total, 12 different mutant receptors were identified, containing altogether 13 mutated positions (**Figure 1**). Amongst the 12 mutant receptors, residues F141$^{4.61}$, C167^{EL2}, and Y202$^{5.58}$ were found mutated more than once. Amino acid changes of F141$^{4.61}$ were identified in two different receptors; in the single mutant F141L$^{4.61}$ and in the double mutant F141C$^{4.61}$/Y202C$^{5.58}$. The mutation C167S^{EL2} was found as a single mutant as well in combination with a residue outside of the cluster: T155^{EL2}. Mutations at position Y202$^{5.58}$ were present in three different mutant receptors: G135A$^{4.55}$/I197L$^{5.53}$/Y202N$^{5.58}$, F141C^{4,61}/Y202C$^{5.58}$, and Y202S$^{5.58}$ (**Table 1**). The mutated residues form three distinct clusters in the receptor; at the top of TM4, at a cysteine-rich area in EL2, and at the bottom of TM5. Four receptors contained mutations in TM4, forming a small cluster of three amino acids: G135$^{4.55}$, I36$^{4.56}$, and F141$^{4.61}$. In EL2 a total of seven residues were found mutated in five different mutant

receptors. Five of the seven residues form a tight cluster, namely $C166^{EL2}$, $C167^{EL2}$, $L168^{EL2}$, $V169^{EL2}$, and $F173^{EL2}$. The cluster seen in TM5 consists of three residues: $I197^{5.53}$, $V200^{5.56}$, and $Y202^{5.58}$ (**Figure 1, Table 1**).

Table 1. Characterization of the adenosine receptor A_{2B} receptor mutants identified from the random mutagenesis screen using the liquid yeast growth assay . Mutations are shown in the numbering of the $A_{2B}R$ protein as well as according to the Ballesteros and Weinstein GPCR numbering system (in superscript). EC_{50} values (nM) are shown as means ± SEM of at least three independent experiments, each performed in duplicate. Results with the ribose agonist NECA are shown for all mutant receptors. For wild type and mutant receptors $F141L^{4.61}$, $C167S^{EL2}$ and $Y202S^{5.58}$ also results with the non-ribose agonist BAY60-6583 are shown. % Emax represents the intrinsic activity of the receptor, where the maximal growth level of wild type receptor in response to the agonists was set as 100%. Fold CA represents the relative increase in growth compared to wild type when no agonist was present.

		NECA 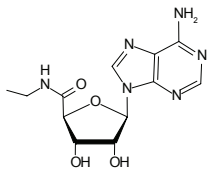		BAY 60-6583 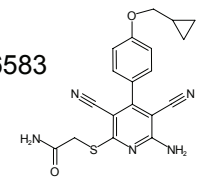	
Mutant	Fold CA	EC_{50} (nM)	% Emax	EC_{50} (nM)	% Emax
WT	1.0	137 +/- 10	100	48 +/- 3	100
$F141L^{4.61}$	1.5	5.4 +/- 0.8	99	9.0 +/- 0.6	102
$C167S^{EL2}$	6.3	8.8 +/- 1.4	100	23 +/- 3	98
$Y202S^{5.58}$	13	13 +/- 3	66	4.9 +/- 0.3	70
$G135A^{4.55}$/$I197L^{5.53}$/ $Y202N^{5.58}$	38	7.1 +/- 0.7	94		
$I136T^{4.56}$	1.5	10 +/- 2	100		
$F141C^{4.61}$/$Y202C^{5.58}$	9.7	15 +/- 2	68		
$S146R^{EL2}$/$V169A^{EL2}$	4.6	9.9 +/- 0.7	101		
$T155A^{EL2}$/$C167S^{EL2}$	3.3	9.3 +/- 1.9	100		
$C166L^{EL2}$	5.6	12 +/- 2	100		
$L168P^{EL2}$	5.5	11 +/- 3	101		
$F173L^{EL2}$	4.2	10 +/- 1	99		
$V200G^{5.56}$	5.0	13 +/- 2	90		

Constitutively active and gain-of-function mutants

To confirm the active phenotype, all 12 receptors were retransformed into the yeast strain and their pharmacology was investigated using yeast-growth assays. All mutant receptors showed an increase in constitutive activity, although less pronounced in mutant receptors F141L$^{4.61}$ and I136T$^{4.45}$ (1.5 times compared to wild type) (**Figure 3A, Table 1**). Mutant receptor G135A$^{4.55}$/I197L$^{5.53}$/Y202N$^{5.58}$ showed the largest increase in basal activity with yeast growth levels 38-fold over wild type, corresponding to 62% of the maximal activation level. The constitutive activity of this mutant receptor could be reduced by the inverse agonist ZM241385, however, a residual activity of 8% remained. The level of constitutive activity of the other 11 mutant receptors could be fully suppressed (**Figure 3A**). For mutant Y202S$^{5.58}$, a full concentration-growth inhibition curve with ZM241385 showed a potency of 31.3 +/- 4.4 nM for ZM241385. In comparison, in literature values between 13 and 50 nM have been reported for wild type A_{2B}R [23,24] (**Figure 3B**).

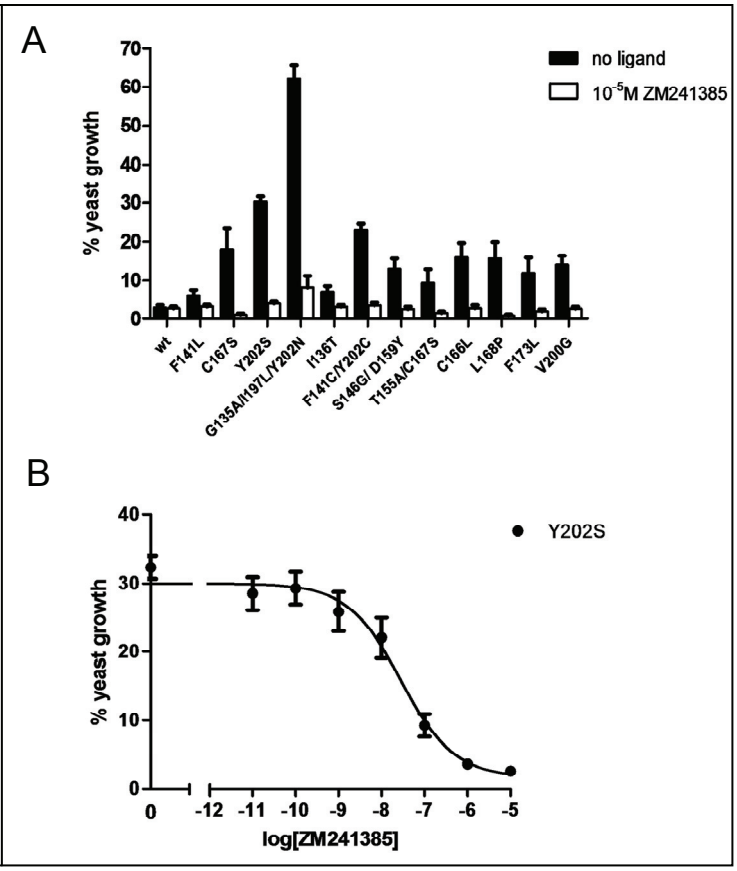

Figure 3. Constitutive activity of the mutant receptors determined in a solid yeast growth assay (*A*) Growth was measured on selective agar plates YNB-ULH in the absence of a ligand or in the presence of 10 µM of the inverse agonist ZM241385. The vertical bars in the graph represent the percentage spontaneous activity of wild type A_{2B}R and mutant receptors (black) and the response to ZM241385 (white). The maximal activation level of wild type receptor was set at 100%, the background of the selection plate was set at 0%. (*B*) Concentration-growth inhibition curve of mutant receptor Y202S$^{5.58}$. A concentration range of 10^{-11} to 10^{-5} M ZM241385 was added to the selection agar plates. The figure is representative of one experiment performed in quadruplicate. The IC_{50} value for ZM241385 was 31.3 +/- 4.4 nM, determined from four independent experiments

Concentration-growth curves revealed that all mutant receptors showed a large increase in potency of more than one log-unit for the full agonist NECA (**Table 1**). Curves of mutant receptors F141L$^{4.61}$, C167S^{EL2}, Y202S$^{5.58}$, G135A$^{4.55}$/I197L$^{5.53}$ /Y202N$^{5.58}$, and T155A^{EL2}/C167S^{EL2} are shown in **Figure 4**. Even though the level of constitutive activity in mutant G135A$^{4.55}$/I197L$^{5.53}$/Y202N$^{5.58}$ was very high, the maximal level of receptor activation could be reached in response to NECA in a dose-dependent manner, with an EC_{50} value of 7.1 +/- 0.7 nM compared to 137 +/- 10 nM seen for wild type $A_{2B}R$ (**Table 1**). Mutant receptor Y202S$^{5.58}$ also has a relatively high level of constitutive activity being 13-fold higher than wild type receptor. However, upon stimulation with NECA the maximum receptor activation (Emax) was lower than observed with wild type $A_{2B}R$. Similar results were observed for the receptor where Y202$^{5.58}$ was mutated in combination with residue F141: mutant receptor F141C$^{4.61}$/Y202C$^{5.58}$ (**Table 1**).

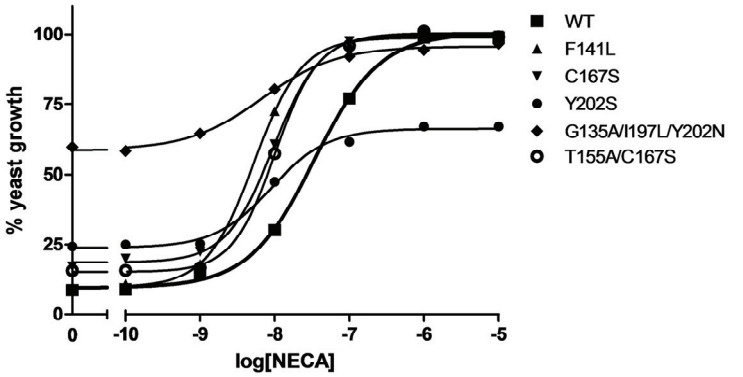

Figure 4.
Concentration- response curves from liquid yeast growth experiments. Curves are shown of wild type (WT ■) and mutant receptors F141L$^{4.61}$ (▲), C167S^{EL2} (▼), Y202S$^{5.58}$ (●), G135A$^{4.55}$/I197L$^{5.53}$/Y202N$^{5.58}$ (♦) and T155A^{EL2}/C167S^{EL2} (○). Curves are shown from a representative experiment. Data for all experiments are presented in Table 1.

Residues F141$^{4.61}$ (TM4), C167^{EL2} (EL2), and Y202$^{5.58}$ (TM5) were identified multiple times in the screen, suggesting a particular important function of these positions in receptor activation. For additional studies, we therefore focused on the single mutant receptors containing each of the residues; F141L$^{4.61}$, C167S^{EL2}, and Y202S$^{5.58}$. These single mutants were also studied with BAY60-6583, a structurally different $A_{2B}R$ agonist [18]. This full agonist lacks a ribose moiety that is present in the adenosine derivative NECA and previously thought to be essential for adenosine receptor activation. The chemical structures of both agonists NECA and BAY60-6583 are shown in **Tables 1 and 2**. BAY60-6583 was more than 5 times more potent at mutant receptor F141L$^{4.61}$; in comparison, NECA's potency was more than 25-fold increased. Both NECA and BAY60-6583 displayed a 10-fold increase in potency on

mutant Y202S$^{5.58}$. Mutant receptor C167S^{EL2} showed a small 2-fold increase in potency in response to BAY60-6583, with NECA this was over 15-fold. Western blot analysis of whole cell lysates showed a similar degree of expression of the mutant receptors compared to the wild type receptor, indicating that the increase in activation profile was not due to overall increases in receptor levels in the system, both intracellular and expressed at the cell surface. Results of mutant receptors F141L$^{4.61}$, C167S^{EL2}, and Y202S$^{5.58}$ are shown in **Figure 5**.

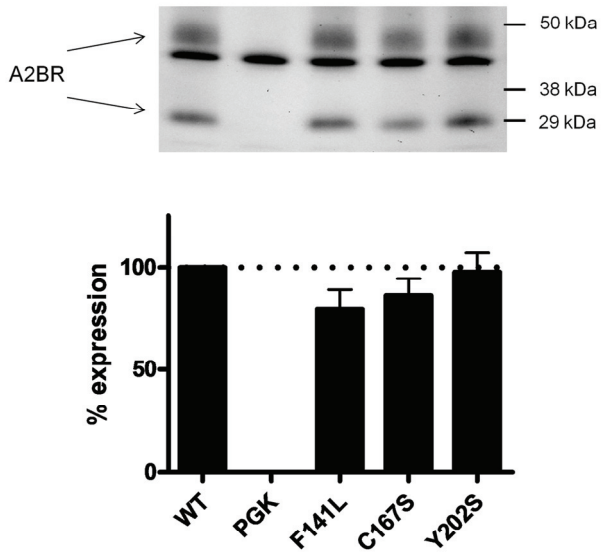

Figure 5. Western Blot Analysis. The relative expression of mutants F141L$^{4.61}$, C167S^{EL2}, Y202S$^{5.58}$ compared to the wild type receptor was determined using densitometric analysis of the Western blots. The ratio was determined between the density of the specific bands and the density of the non-specific band that is always present on the blot. Wild type receptor was set at 100%, the empty vector pDT-PGK was set at 0%. The experiment was performed in duplicate. One representative blot is shown in the upper panel. The arrows indicate the specific $A_{2B}R$ bands; these are located at ca. 29 kDa and 48 kDa.

Radioligand binding experiments on the activated mutant receptors

To investigate the influence of the mutated residues on binding next to activation, we performed radioligand binding experiments using the $A_{2B}R$ selective antagonist [^{3}H]PSB-603 [3,20]. Saturation binding experiments showed a K_D of the radioligand on whole yeast cells expressing the $hA_{2B}R$ of 0.81 +/- 0.02 nM (data not shown), in comparison, the K_D value determined on CHO cell membranes expressing the $hA_{2B}R$ was 0.40 +/- 0.19 nM [20]. Competition binding curves were made for wild type and mutant receptors with unlabeled NECA, BAY 60-6583, or ZM241385 as a displacer. For mutant receptor Y202S$^{5.58}$ we were not able to reach a high enough window to perform competition binding curves. This is likely due to a decrease in affinity for the radiolabeled antagonist [^{3}H]PSB-603 since no change in expression levels was observed (**Figure 5**).

Table 2. Competition binding experiments with the radiolabeled antagonist [^{3}H]PSB-603 ($K_{D,yeast}$ = 0.8 +/- 0.02 nM). Mutants F141L$^{4.61}$ and C167S^{EL2} were tested on their affinity for the full agonist NECA, the non-ribose agonist BAY 60-6583, and the inverse agonist ZM241385. IC_{50} values are shown as means ± SEM of at least three independent experiments, each performed in duplicate.

	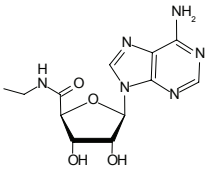	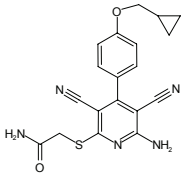	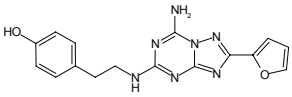
	IC_{50} (nM) NECA	IC_{50} (nM) BAY 60-6583	IC_{50} (nM) ZM241385
WT	1574 +/ 411	785 +/- 74	58 +/- 5
F141L$^{4.61}$	123 +/- 18	137 +/- 8	87 +/- 2
C167S^{EL2}	173 +/- 33	818 +/- 82	104 +/- 18

Mutant receptors F141L$^{4.61}$ and C167S^{EL2} showed a large increase in NECA affinity compared to the wild type receptor of 13-fold and 9-fold, respectively (**Table 2**). In the radioligand binding experiment with BAY 60-6583 as displacer, the affinity of mutant F141L$^{4.61}$ was again increased. In contrast, mutant C167S^{EL2} had an affinity for BAY 60-6583 similar to wild type A_{2B} receptor (**Figure 6, Table 2**). The affinity of the inverse agonist ZM241385 was also determined. Both mutant receptors did not show a large change in affinity for ZM241385 compared to wild type receptor, although the effect on F141L$^{4.61}$ was significant (**Table 2**).

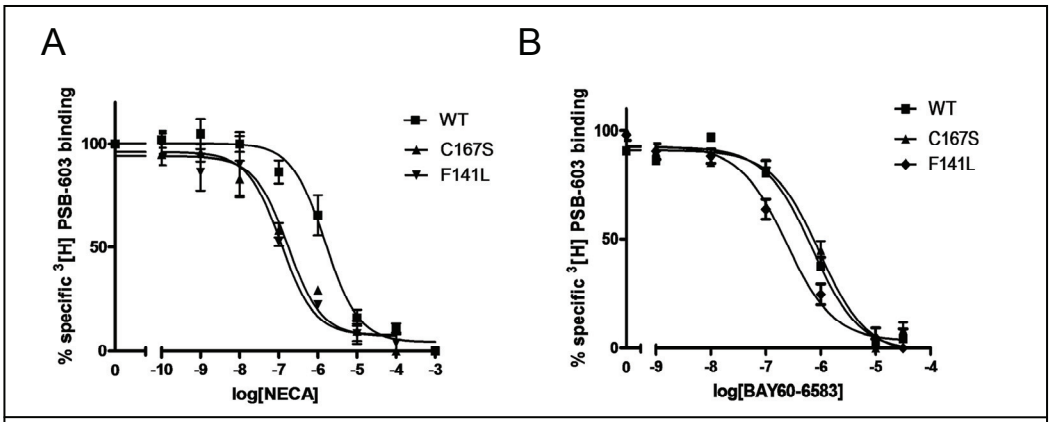

Figure 6. Competition binding curves using [^{3}H]PSB-603. (*A*) Displacement curves of wild type $A_{2B}R$ (■) and mutant receptor C167S^{EL2} (▲) with the ribose agonist NECA. (*B*) Displacement curves of wild type $A_{2B}R$ (■) and mutant receptor C167S^{EL2} (▲) with the non-ribose agonist BAY 60-6583. The graphs are the combined result of three independent experiments performed in duplicate.

Bioinformatic analyses

Recently, several crystal structures of the adenosine A_{2A} receptor have been elucidated (PDB entry codes: 3EML, 3QAK, 2YDO, 2YDV) [5,6,7]. The adenosine A_{2A} receptor is the closest homologue of the adenosine A_{2B} receptor, with 82.1 % amino acid similarity and 59.4 % identity. We mapped the mutated residues onto the crystal structure of the active A_{2A}R structure bound to NECA (PDB: 2YDV) in order to obtain a view on the 3D localization of the residues (**Figure 7**). The corresponding positions of the mutated A_{2B}R residues in the A_{2A}R sequence were determined by a multiple sequence alignment (**Figure 7A**). To improve the quality of the multiple sequence alignment and to determine the transition between loop and transmembrane domains, we also included sequences of two other crystallized GPCRs; the β_2-adrenergic (b2AR) receptor and the CXCR4 Chemokine (CXCR4R) receptor [25,26]**.** Also in the 3D view, clusters of mutations can be observed in the top of TM4 and the bottom of TM5 (**Figure 7B**). The corresponding positions of the cluster in EL2 appear to reside in a part of the loop that is involved in forming an anti-parallel β-sheet with EL1. It is very likely that this typical protein structure is also present in the A_{2B}R and constitutively active mutations in the putative β-strand in EL1 of this receptor have previously been described by our laboratory [3].

In the A_{2A} receptor structure, all three available cysteines in the second extracellular loop are involved in bridge formation. It has been proposed that formation of extracellular disulfide bridges may be an important general mechanism for regulating the activity of GPCRs [27]. The adenosine A_{2B}R has a high number of cysteines in EL2 that could all potentially form extracellular disulfide bridges. A previous sequence alignment analysis performed by De Graaf et al. already revealed that over 90% of class A GPCRs contain at least one cysteine in EL2 and that several receptors contain more. In most cases, the most downstream cysteine appeared involved in forming the conserved disulfide bridge with TM3 [28]. To investigate how common multiple cysteines are in class A GPCRs, we performed a cysteine occurrence analysis. We counted the number of cysteines present between residues 4.55 and 5.38 [21], a region that encompasses the second extracellular loop. The majority of non-olfactory receptors contains only one cysteine within EL2 (**Figure 8A**); this cysteine represents in most cases the conserved cysteine present in over 90% of class A GPCRs. From what is known from the currently available crystal structures this conserved cysteine forms a disulfide bridge with a cysteine present in the top of

TM3 that is essential for receptor structure and function. The adenosine $A_{2B}R$ is the only receptor with four cysteines in EL2, which is the highest cysteine count in this analysis. The adenosine A_{2A} receptor, the closest homologue of the $A_{2B}R$, contains one cysteine less with three cysteines in the loop. The other adenosine receptor subtypes, the A_1R and A_3R, only hold one cysteine in EL2. In EL2 of olfactory receptors, generally multiple cysteines are present; ca. 80% of the receptors contain three cysteines in the loop (**Figure 8B**). This special subfamily of class A GPCRs is responsible for our sense of smell by binding odorants. Metal ions, such as zinc, have been proposed to be essential in recognition and binding of odorants to their receptor, in which ligation of the metal ion to the thiol group of cysteine residues might play an important role [29].

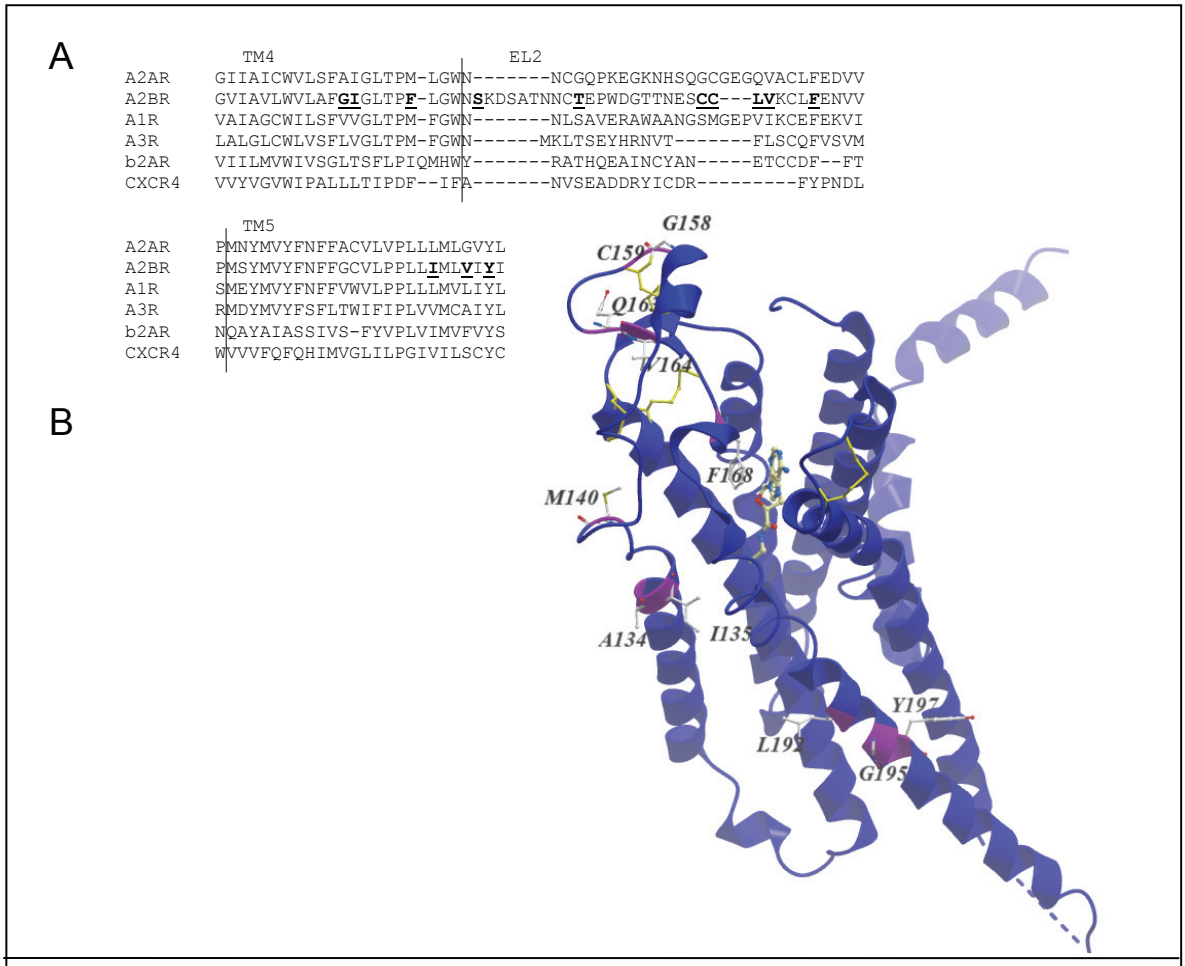

Figure 7. Mutated residues of the $A_{2B}R$ mapped on the crystal structure of the $A_{2A}R$.
(*A*) Multiple sequence alignment $A_{2B}R$ with all four adenosine receptor subtypes ($A_{2A}R$, $A_{2B}R$, A_1R, A_3R) as well as the sequences of two other crystal structures of CXCR4 and the β_2-adrenergic receptor (b2AR) to ensure the most plausible definition of EL2. The mutated residues are indicated in bold font and underlined. (*B*) Based on the multiple sequence alignment, the mutated residues identified in the random mutagenesis screen were mapped onto the crystal structure of the $A_{2A}R$ (PDB: 2YDV) (blue), the closest homologue of the $A_{2B}R$. The corresponding mutated residues and their side-chains are indicated in magenta. The ribbon representation also shows the co-crystallized ligand NECA as well as the three disulfide bridges that restrict EL2 in the A_{2A} receptor

DISCUSSION

A random mutagenesis screen for gain-of-function and constitutively active mutants (CAMs) was performed on fragment TM4-EL2-TM5 of the human adenosine A_{2B} receptor. These three regions of the receptor have been implied to participate in the dynamic movements the receptor undergoes during activation. Upon receptor activation, a coupling between movements of EL2 and TM5 has been observed as well as a rearrangement in the hydrogen-bonding networks connecting EL2 with the extracellular ends of TM4, TM5 and TM6 [4].

For the β_1-adrenergic receptor, the β_2-adrenergic receptor, (rhod)opsin, and the adenosine A_{2A} receptor, we now have access to crystal structures of both inactive and active conformations [5,6,7,30,31,32,33,34,35]. These structures reveal that in the transition between the inactive and the active conformation subtle changes at the extracellular surface and the ligand binding site lead to large movements at the intracellular surface. The lower regions of TM5 and TM6 show a particularly large displacement that is allowed by the presence of conserved prolines (5.50 and 6.50) that interrupt the hydrogen bond network within the helices.

From the screen, 12 different mutant receptors were identified. Most of these mutants show a significant increase in constitutive activity, with mutant G135A$^{4.55}$ /I197L$^{5.53}$/Y202N$^{5.58}$ even reaching a basal activity that is over 60% of the maximal activation level (**Figure 3**). All mutant receptors displayed a very large increase in potency for NECA compared to wild type, ranging from an improvement in activation of 11-fold (V200G$^{5.56}$) to even 25-fold (F141L$^{4.61}$) (**Table 1**). That we were able to identify mutant receptors with such large effects on activation further emphasizes the strength of using an unbiased random mutagenesis approach in combination with the *S. cerevisiae* system.

Three "hotspots" important for A_{2B}R activation

The residues found mutated in our screen are located in three distinct clusters: at the top of TM4, in a cysteine-rich region in EL2, and at the bottom half of TM5 (**Figures 1 and 7B**). Even though a number of mutant receptors contain multiple amino acid changes, no combinations between mutations in EL2 and the transmembrane domains were identified. This suggests that the influence of EL2 on receptor activation is at a different level than that of the transmembrane domains. There is

accumulating evidence that agonist binding and activation occur through a series of conformational intermediates, for which multiple switches are needed to be activated [36,37]. It is quite likely that the first switch is present at the site of ligand entry to the receptor, i.e. at the extracellular surface.

The cluster in TM4 consists of three amino acids; $G135^{4.55}$, $I136^{4.56}$, and $F141^{4.61}$. A saturated mutagenesis screen performed on the transmembrane domains of the complement factor 5a receptor (C5aR), also revealed important residues at the extracellular membrane interface of TM4, corresponding to positions 4.46, 4.53, 4.55, 4.57, 4.58, and 4.60 [38,39]. Very recently, Warne et al. published four structures of the β_1-adrenergic receptor bound to full and partial agonists. One difference between an antagonist and a full agonist bound β_1-adrenergic receptor is that a Van der Waals interaction is broken between positions 4.56 and 5.46. This results in a reduced interface between helix 4 and 5 that may be significant in the activation process [30]. In the inactive structure of the adenosine A_{2A} receptor (PDB:3EML), a similar Van der Waals interaction exists between $I135^{4.56}$ and $C185^{5.46}$. Also, a hydrogen bond is formed between $Q89^{3.37}$ and the backbone of $C185^{5.46}$ [5]. In the active structures of the $A_{2A}R$ (PDB: 3YDO/3YDV/ 3QAK), the cysteine side chain shifts and the hydrogen bond is broken [6,7]. Noteworthy is that in the 3YDO and 3YDV structures bound to adenosine and NECA respectively, position 3.37 was mutated (Q89A) [7].

The mutations found mutated in EL2 are located in a cysteine-rich region of the loop that may be involved in a β-strand structure in the loop as is seen in the structure of the $A_{2A}R$ (**Figure 7B**). The partnering strand in EL1 that is involved in forming the β-sheet with EL2, has previously been reported to be essential in $A_{2B}R$ activation [3]. EL2 has been suggested to act as a negative regulator that keeps the receptor in a silent state before agonist-induced activation [8,9,10]. The mutant receptors in EL2 that we identified all showed a large increase in receptor activation, both in response to the agonist NECA and independent of a ligand. This could suggest that the cysteine-rich cluster we identified in our screen has a similar regulating role in suppressing receptor activation in its basal state. The cysteine occurrence analysis on all human class A GPCRs revealed that the $A_{2B}R$ contains an exceptionally large number of four cysteines in EL2, whereas most non-olfactory class A GPCRs only contain one cysteine (**Figure 8**; see also an analysis by De Graaf et al., 2008) [28]. In

olfactory receptors the cysteine occurrence is much higher, which may be linked to metal ion binding [29].

In TM5, the mutated residues are found in a small cluster of three residues at the bottom of the helix: I197$^{5.53}$, V200$^{5.56}$, and Y202$^{5.58}$. From the crystal structure of the A_{2A}R, as well as additional mutagenesis data, several residues in TM5 have been indicated to play a role in agonist and/or antagonist binding: M177$^{5.38}$, F180$^{5.41}$, N181$^{5.42}$, and F182$^{5.43}$ [5,40]. The recently published active structures in which NECA and adenosine are co-crystallized, reveal that M177$^{5.38}$, N181$^{5.42}$ are directly involved in the ligand binding pocket of these ribose-containing agonists [7]. The residues identified in our screen are located much lower in the helix and are therefore unlikely to participate in the ligand binding pocket. However, the large increase in agonist potency and constitutive activity observed in our study implies that these residues are essential in receptor activation.

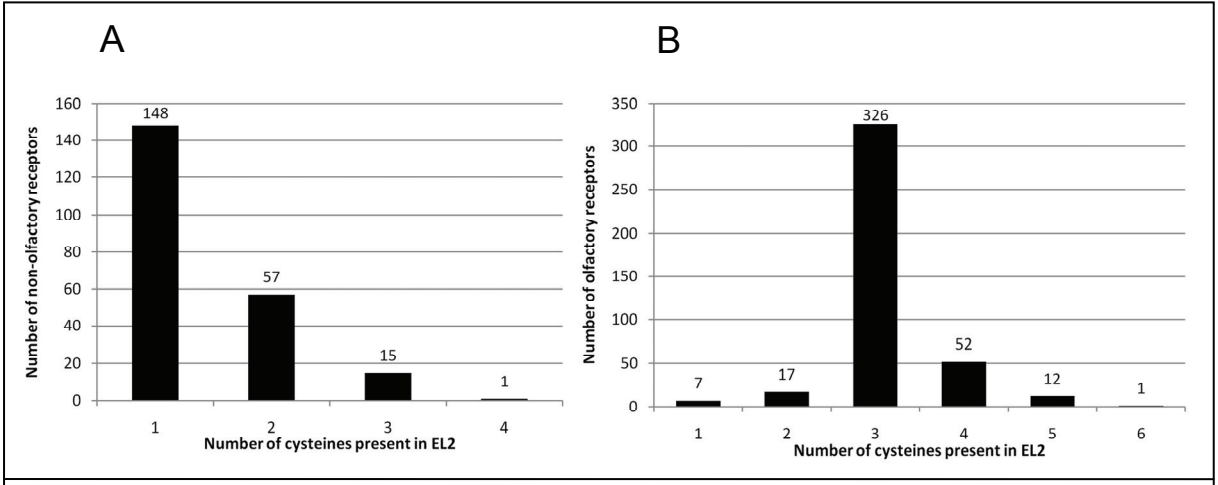

Figure 8. Cysteine occurrence analysis. The number of cysteines present in the second extracellular loop was counted in human class A GPCRS. For this analysis, the loop was defined between residues 4.55 (TM4) and 5.38 (TM5). The graphs represent all human class A GPCRs, either non-olfactory (*A*) or olfactory (*B*), as present in the GPCRDB (http://www.gpcr.org/7tm/), with on the x-axis the number of cysteines counted in EL2. The majority of non-olfactory receptors contains one cysteine in EL2, the adenosine A_{2B} receptor alone is responsible for the bar at 4 cysteines. Most olfactory receptors have three cysteines in the loop

CAMs in the adenosine A_{2B} receptor

The fragments upstream and downstream of the investigated fragment TM4-EL2-TM5 had been subjected to a random mutagenesis screen in a similar manner in our laboratory [2,3]. In **Figure 1**, the ensemble of CAM residues identified in the different studies is indicated in grey, from which we conclude that next to the described clusters in TM4, EL2, and TM5, similar series of residues exist in TM3 and TM6.

Even though the screening set up in all three screens (ATG-KpnI, TM4-EL2-TM5, and BglII-stop) was chosen such that both constitutively active mutants (CAMs) and gain-of-function mutants would be selected, all the identified mutant receptors displayed an increase in constitutive activity. The levels of constitutive activity ranged from a 1.5-fold change (F141L$^{4.61}$, N36D^{IL1}) compared to wild type receptor to an immense increase of 38-fold for mutant receptor G135A$^{4.55}$/I197L$^{5.53}$/Y202N$^{5.58}$. Interestingly, of all 41 residues identified in constitutively active mutants of the $A_{2B}R$, only 4 were actually involved in binding of either adenosine or NECA at the corresponding positions in the crystal structures of the $A_{2A}R$ published by Lebon et al.[7] These corresponding residues in the $A_{2B}R$ are: F173^{EL2}, V250$^{6.51}$, N254$^{6.55}$ and T257 $^{6.58}$. The last three, all residing in TM6, were identified in one particular multiple mutant receptor; Q214L/I230N/V240M/V250M/N254Y/T257S/K269stop (IL3/6.31 /6.41/6.51/6.55/6.58/EL3) [2]. The residue F173^{EL2} (F168 in $A_{2A}R$) directly interacts with all the ligands co-crystallized with the $A_{2A}R$ through a π-stacking contact. For the antagonist ZM241385 the triazolotriazine ring interacts with the phenylalanine, where in the agonists UK-432097, NECA, and adenosine, π-stacking occurs with the adenine moiety. In the study described here, the F173L^{EL2} mutant receptor displayed a large increase in potency for NECA. Mutating the corresponding F168^{EL2} in the $A_{2A}R$ into other aromatic residues resulted in a moderate decrease in activation of the receptor, mutation into an alanine virtually abolished activation [40]. Assuming that the F173^{EL2} in the $A_{2B}R$ has a similar role in binding, a large hydrophobic residue might be required at this position, however removing the aromatic side chain can even improve agonist access to the binding pocket.

Many of the CAMs in our studies only have one or two amino acid changes, indicating that quite subtle changes can lead to a large impact on the receptor activation mechanism and that these residues are not necessarily directly involved in either ligand binding or G protein-coupling.

Residues F141$^{4.61}$, C167^{EL2}, and Y202$^{5.58}$

The amino acids F141$^{4.61}$, C167^{EL2}, an Y202$^{5.58}$ were identified multiple times in the screen. This may indicate that these residues are of particular importance in the activation mechanism of the $A_{2B}R$. Position F141$^{4.61}$ has been reported previously as being involved in affinity and potency changes. The polymorphic variant M172I$^{4.61}$,

located at the corresponding position in the serotonin 1A receptor (5HT1A), displayed a 3-fold increase in agonist potency [41]. In another subtype of serotonin receptors, 5HT1B, substitution of the amino acid F185$^{4.61}$ by an alanine increased the affinities for several agonists [42]. In the study described here, mutating F141$^{4.61}$ to a leucine resulted in a 25-fold increase in potency for NECA and a 5-fold increase in potency in response to the non-ribose agonist BAY60-6583 (**Figure 2, Table 1**). Radioligand binding studies revealed that affinity for both agonists was also largely increased (**Table 2**). The residue is located at the onset of EL2, pointing outwards (**Figure 7B**). Although the residue is at great distance from the putative binding pocket of both NECA and BAY60-6583, it is firmly involved in both agonist activation and binding [43]. The location of the residue does suggest a main role in positioning EL2, and could therefore be indirectly involved in shaping the entry of the agonist binding pocket.

Mutant receptor C167S^{EL2} showed an increase of ca. 16-fold in potency for the adenosine derivative NECA as well as a constitutive activity that was 6-fold higher compared to wild type (**Table 1**). Radioligand binding experiments also revealed an increase in binding affinity for the adenosine derivative NECA (**Figure 5**). Interestingly, when we activated the C167S^{EL2} mutant with BAY 60-6583, a structurally different agonist that lacks a ribose moiety, only a 2-fold change in potency was observed and affinity remained unchanged compared to wild type (**Figure 5, Table 1**). Residue C167^{EL2} is likely able to form a non-conserved disulfide bridge with a cysteine in EL1 in the A_{2B}R as seen in the crystal structure of the closest family member, the A_{2A}R [3] (**Figure 1**). Our results indicate that the putative disulfide bridge between C167^{EL2} and C72^{EL1} is important for ribose agonist binding and activation, but less so for non-ribose agonists. Schiedel et al. recently performed a site-directed mutagenesis study on the cysteine residues present in EL2 of the A_{2B}R. Mutating C167^{EL2} to a serine resulted in a 2.5-fold increase in potency for BAY60-6583, similar to our observations, although the response to NECA of this mutant receptor was less pronounced in their study [44]. The tyrosine at position 202$^{5.58}$ is highly conserved among class A GPCRs (88%) and there are several studies reporting this position as being important in receptor activation and G protein signaling. A somatic mutation in the thyroid stimulating hormone receptor (TSHR) involved in toxic adenoma, Y601N$^{5.58}$, showed increased levels of constitutive activity, but was unable to couple to Gq/11 [45]. Very recently, Sansuk et al.

proposed that movement at the extracellular side of TM5 is transduced as a set of structural rearrangements toward the intracellular side, so enabling interactions of Y5.58 with R3.50 in the cytoplasmic side of the receptor [46]. When comparing the inactive and active structures of the adenosine A_{2A} receptor, we learned that Y5.58 (Y197 in the $A_{2A}R$) displays a large rotameric shift upon activation. While in the inactive structure bound to ZM241385 the conserved $Y197^{5.58}$ is located in between TM3 and TM6, in the agonist-bound forms this residue moves outward allowing TM5 to shift toward TM6. As a result, the intracellular ends of TM5 and TM6 move closer together in the active structures compared to the inactive structure, enabling access of the G protein [5,6,7]. In our screen, mutant $Y202S^{5.58}$ showed a 13-fold increase in constitutive activity that could be reduced to wild type levels in response to the inverse agonist ZM241385 with an IC_{50} comparable to the wild type receptor, indicating that the mutation does not lock the receptor in an active conformation [23,24] **(Figure 3**). NECA potency was 11-fold increased, but maximal activation levels could not be reached, suggesting a decrease in coupling to and signaling through the G protein (**Figure 2, Table 1**).

Concluding remarks

By applying an unbiased random mutagenesis approach with subsequent phenotype screening in a robust yeast system, we identified three hotspots in the $A_{2B}R$ that show a vast increase in both spontaneous and agonist-induced activity. None of the identified residues within these three clusters are part of the ligand binding pocket, yet, they are involved in agonist potency and affinity. Some of the identified residues, like $C167^{EL2}$, most likely contribute to an $A_{2B}R$-specific response to agonists. Others, such as $F141^{4.61}$ and $Y202^{5.58}$, might be part of a general activation mechanism for class A GPCRs. An overview of all the CAMs in the $A_{2B}R$ identified so far, indicates that there are several clusters of amino acids responsible for maintaining the subtle equilibrium that exist between the active conformation R^* and the inactive conformation R of the receptor and that these residues are not necessarily directly involved in either ligand binding or G protein coupling. In more general terms the results presented here could be of great use in unraveling the molecular details of GPCR activation.

ACKNOWLEDGEMENTS

This research was performed under the auspices of the GPCR Forum, a program funded by the Dutch Top Institute Pharma (project D1-105). The authors thank Bas Vroling and the GPCRDB (http://www.gpcr.org/7tm/) for help with the cysteine occurrence analysis. They also are greatly indebted to Prof C.E. Müller of Bonn University for the gift of [^{3}H]PSB-603.

REFERENCES

[1] Fredholm, B.B., IJzerman, A.P., Jacobson, K.A., Linden, J., Muller, C.E., *Pharmacol Rev* (2011) 63:1-34.
[2] Beukers, M., van Oppenraaij, J., van der Hoorn, P., Blad, C., den Dulk, H., Brouwer, J., IJzerman, A., *Mol Pharmacol.* (2004) 65:702-710.
[3] Peeters, M.C., van Westen, G.J., Guo, D., Wisse, L.E., Muller, C.E., Beukers, M.W., IJzerman, A.P., *FASEB J* (2011) 25:632-643.
[4] Ahuja, S., et al., *Nat Struct Mol Biol* (2009) 16:168-175.
[5] Jaakola, V.P., Griffith, M.T., Hanson, M.A., Cherezov, V., Chien, E.Y., Lane, J.R., IJzerman, A.P., Stevens, R.C., *Science* (2008) 322:1211-1217.
[6] Xu, F., Wu, H., Katritch, V., Han, G.W., Jacobson, K.A., Gao, Z.G., Cherezov, V., Stevens, R.C., *Science* (2011).
[7] Lebon, G., Warne, T., Edwards, P.C., Bennett, K., Langmead, C.J., Leslie, A.G., Tate, C.G., *Nature* (2011) 474:521-525.
[8] Klco, J., Wiegand, C., Narzinski, K., Baranski, T., *Nat Struct Mol Biol.* (2005) 12:320-326.
[9] Massotte, D., Kieffer, B.L., *Nat Struct Mol Biol* (2005) 12:287-288.
[10] Peeters, M.C., van Westen, G.J., Li, Q., IJzerman, A.P., *Trends Pharmacol Sci* (2011) 32:35-42.
[11] Jaakola, V.P., IJzerman, A.P., *Curr Opin Struct Biol* (2010) 20:1-14.
[12] Smit, M., Vischer, H., Bakker, R., Jongejan, A., Timmerman, H., Pardo, L., Leurs, R., *Annu Rev Pharmacol Toxicol.* (2007) 47:53-87.
[13] Brown, A., et al., *Yeast* (2000) 16:11-22.
[14] Stewart, G.D., Valant, C., Dowell, S.J., Mijaljica, D., Devenish, R.J., Scammells, P.J., Sexton, P.M., Christopoulos, A., *J Pharmacol Exp Ther* (2009) 331:277-286.
[15] Fromant, M., Blanquet, S., Plateau, P., *Anal Biochem* (1995) 224:347-353.
[16] Beukers, M., IJzerman, A., *Trends Pharmacol Sci.* (2005) 26:533-539.
[17] Gietz, D., St Jean, A., Woods, R.A., Schiestl, R.H., *Nucleic Acids Res* (1992) 20:1425.
[18] Eckle, T., et al., *Circulation* (2007) 115:1581-1590.
[19] Li, Q., Ye, K., Blad, C.C., den Dulk, H., Brouwer, J., IJzerman, A.P., Beukers, M.W., *J Pharmacol Exp Ther* (2007) 320:637-645.
[20] Borrmann, T., Hinz, S., Bertarelli, D.C., Li, W., Florin, N.C., Scheiff, A.B., Muller, C.E., *J Med Chem* (2009) 52:3994-4006.
[21] Ballesteros, J.A., Weinstein, H., *Methods Neurosci* (1995) 25:366–428.
[22] Vroling, B., Sanders, M., Baakman, C., Borrmann, A., Verhoeven, S., Klomp, J., Oliveira, L., de Vlieg, J., Vriend, G., *Nucleic Acids Res* (2011) 39:D309-319.
[23] de Zwart, M., Vollinga, R.C., Beukers, M.W., Sleegers, D.F., Kunzel, J.K.V.D., de Groote, M., IJzerman, A.P., *Drug Development Research* (1999) 48:95-103.
[24] Ongini, E., Dionisotti, S., Gessi, S., Irenius, E., Fredholm, B.B., *Naunyn Schmiedebergs Arch Pharmacol* (1999) 359:7-10.
[25] Wu, B., et al., *Science* (2010) 330:1066-1071.
[26] Rosenbaum, D.M., et al., *Science* (2007) 318:1266-1273.
[27] Storjohann, L., Holst, B., Schwartz, T.W., *Biochemistry* (2008) 47:9198-9207.
[28] de Graaf, C., Foata, N., Engkvist, O., Rognan, D., *Proteins* (2008) 71:599-620.
[29] Wang, J., Luthey-Schulten, Z.A., Suslick, K.S., *Proc Natl Acad Sci U S A* (2003) 100:3035-3039.

[30] Warne, T., Moukhametzianov, R., Baker, J.G., Nehme, R., Edwards, P.C., Leslie, A.G., Schertler, G.F., Tate, C.G., *Nature* (2011) 469:241-244.
[31] Park, J.H., Scheerer, P., Hofmann, K.P., Choe, H.W., Ernst, O.P., *Nature* (2008) 454:183-187.
[32] Rasmussen, S.G., et al., *Nature* (2011) 469:175-180.
[33] Rasmussen, S.G., et al., *Nature* (2007) 450:383-387.
[34] Palczewski, K., et al., *Science* (2000) 289:739-745.
[35] Warne, T., Serrano-Vega, M.J., Baker, J.G., Moukhametzianov, R., Edwards, P.C., Henderson, R., Leslie, A.G., Tate, C.G., Schertler, G.F., *Nature* (2008) 454:486-491.
[36] Kobilka, B.K., Deupi, X., *Trends Pharmacol Sci* (2007) 28:397-406.
[37] Ahuja, S., Smith, S.O., *Trends Pharmacol Sci* (2009) 30:494-502.
[38] Baranski, T., Herzmark, P., Lichtarge, O., Gerber, B., Trueheart, J., Meng, E., Iiri, T., Sheikh, S., Bourne, H., *J Biol Chem.* (1999) 274:15757-15765.
[39] Geva, A., Lassere, T.B., Lichtarge, O., Pollitt, S.K., Baranski, T.J., *J Biol Chem* (2000) 275:35393-35401.
[40] Jaakola, V.P., Lane, J.R., Lin, J.Y., Katritch, V., IJzerman, A.P., Stevens, R.C., *J Biol Chem* (2010) 285:13032-13044.
[41] Del Tredici, A.L., Schiffer, H.H., Burstein, E.S., Lameh, J., Mohell, N., Hacksell, U., Brann, M.R., Weiner, D.M., *Biochem Pharmacol* (2004) 67:479-490.
[42] Granas, C., Nordvall, G., Larhammar, D., *Eur J Pharmacol* (1998) 349:367-375.
[43] Sherbiny, F.F., Schiedel, A.C., Maass, A., Muller, C.E., *J Comput Aided Mol Des* (2009) 23:807-828.
[44] Schiedel, A.C., Hinz, S., Thimm, D., Sherbiny, F., Borrmann, T., Maass, A., Muller, C.E., *Biochem Pharmacol* (2011) 82(4):389-99.
[45] Arseven, O.K., Wilkes, W.P., Jameson, J.L., Kopp, P., *Thyroid* (2000) 10:3-10.
[46] Sansuk, K., Deupi, X., Torrecillas, I., Jongejan, A., Nijmeijer, S., Bakker, R., Pardo, L., Leurs, R., *Mol Pharmacol* (2011) 79:262-269.